J. H. LIENHARD
Professor.
Mem. ASME

V. K. DHIR
Research Assistant.
Student Mem. ASME

Boiling and Phase Change Laboratory,
Mechanical Engineering Department,
University of Kentucky,
Lexington, Ky.

Hydrodynamic Prediction of Peak Pool-boiling Heat Fluxes from Finite Bodies[1]

Since Zuber made a hydrodynamic prediction of the peak pool-boiling heat flux on an infinite flat plate, his general concept has been used to predict the peak heat flux in two finite heater configurations. These latter predictions have differed from Zuber's in the introduction of a largely empirical variable—the thickness of the vapor escape path around the body. The present study shows how measurements of this thickness can be combined with the hypothesis that the vapor velocity within the vapor blanket must match the vapor velocity in the escaping jet above the heater. The result is a more exact description of the hydrodynamics of vapor removal. This idea is used to suggest the possibility of a universal value for the ratio of the cross-sectional area of escaping jets to the heater area for large finite heaters and for long slender heaters. A set of general ground rules is developed for predicting the peak heat fluxes on both large and small heaters. These rules are used in turn to predict the peak heat flux from horizontal ribbons. They are also used to correct the traditional prediction for infinite-flat-plate heaters. The predictions are supported with new data.

Introduction

THE HYDRODYNAMIC theory of Zuber and Tribus [1, 2][2] showed rationally, in 1958, why the older correlative equation of Kutateladze [3] was the correct expression for the peak pool-boiling heat flux q_{max} on an infinite horizontal flat plate. In the early 1960s Kutateladze and his co-workers began [4] a research effort aimed at correlating q_{max} on horizontal cylinders. In 1964 and 1965 respectively they [5] and Lienhard and Watanabe [6] showed that q_{max} data for cylinders (and other geometries) could be correlated with an expression of the form

$$\frac{q_{max}}{q_{max_F}} = f(L') \tag{1}$$

where q_{max_F} is the "traditional" or accepted form of Zuber's expression for q_{max} on horizontal flat-plate heaters[3]

$$q_{max_F} \equiv \frac{\pi}{24}\,\rho_g{}^{1/2} h_{fg}[\sigma g(\rho_f - \rho_g)]^{1/4} \tag{2}$$

and L' is a nondimensionalization of the characteristic length L of the heater

$$L' \equiv L\sqrt{g(\rho_f - \rho_g)/\sigma} \tag{3}$$

The restrictions on equation (1) are discussed fully in [7]. Briefly: the pressure must be enough less than the critical pressure that $\rho_g/\rho_f \ll 1$; the body must be shaped so that fluid motion induced by the rising bubbles draws liquid around (rather than into) the bubble escape path; and the surface must be clean.

During the past four years this laboratory has been involved in formulating hydrodynamic predictions of q_{max} on a variety of finite heaters. In 1970 a hydrodynamic theory for q_{max} on horizontal cylinders was derived by Sun [8]. Ded [9] subsequently provided a prediction of q_{max} on spheres. Both [8] and [9] required the evaluation of a "vapor-blanket thickness" δ. This δ was the thickness of the vapor escape passage around the body, and it generally appeared that experimental data had to be used in its evaluation.

In the present study we shall show how the previous models can be treated using less empirical information than before. We shall infer from these models some general features of any hydrodynamic prediction and so eliminate the need for observed values of δ. Finally we shall use these ideas in the prediction of q_{max} expressions for some new configurations and verify these expressions with new data.

Previous Theoretical Models

Zuber's original formulation began quite simply with the proposition that the maximum or limiting vapor volume flux is

[1] This work was performed with the support of NASA grant NGR-18-001-035 under the cognizance of the Lewis Research Center.
[2] Numbers in brackets designate References at end of paper.
[3] Symbols not explained in the text are ones in common use; they are defined in the Nomenclature.

Contributed by the Heat Transfer Division and presented at the Winter Annual Meeting, New York, N. Y., November 26–30, 1972, of THE AMERICAN SOCIETY OF MECHANICAL ENGINEERS. Manuscript received by the Heat Transfer Division November 12, 1971. Paper No. 72-WA/HT-10.

$$q_{\max}/\rho_g h_{fg} = U_H \frac{A_j}{A_h} \tag{4}$$

in which A_j is the combined area of vapor jets leaving a heater surface of area A_h. U_H is the critical vapor velocity within the jets which will cause them to become Helmholtz unstable. Equation (4) is the starting point for everything we shall do here. Each prediction brings with it two component problems which must be solved: A vapor jet configuration must be assumed in order to specify A_j/A_h, and the critical velocity must be obtained. The latter can be shown (see, e.g., [10] page 462 or [11]) to be

$$U_H = \sqrt{2\pi\sigma/\rho_g \lambda_H} \tag{5}$$

where λ_H is the wavelength of the disturbance that gives rise to the instability in the vapor–liquid interface of the jet. Substituting equation (5) in equation (4) and introducing equation (2) we obtain

$$\frac{q_{\max}}{q_{\max F}} = \frac{24}{\pi} \sqrt{\frac{2\pi}{\lambda_H \sqrt{g(\rho_f - \rho_g)/\sigma}}} \frac{A_j}{A_h} \tag{6}$$

Infinite Horizontal Flat Plate. Zuber's original derivation of $q_{\max F}$ involved a number of assumptions which we shall want to modify here. Hence we shall speak of $(q_{\max})_{\text{flat plate}}$, which may or may not equal $q_{\max F}$. Nevertheless there is now considerable historical precedent for using $q_{\max F}$ as defined by equation (2) in the functional equation (1). Accordingly we shall adopt the view that $q_{\max F}$ is a *characteristic heat flux* which approximates $(q_{\max})_{\text{flat plate}}$.

Zuber reasoned that (in the absence of any geometrical features of the heater) the jets of escaping vapor would form on the nodes of the square two-dimensional grid of collapsing Taylor-unstable waves as illustrated at the top of Fig. 1. At the time he could provide no basis for selecting either the minimum unstable Taylor wavelength[4]

$$\lambda_c = 2\pi\sqrt{\sigma/g(\rho_f - \rho_g)} \tag{7}$$

or the most susceptible, or "most dangerous," wavelength[4]

$$\lambda_d = 2\pi\sqrt{3}\,\sqrt{\sigma/g(\rho_f - \rho_g)} = \sqrt{3}\,\lambda_c \tag{8}$$

Subsequent work with film boiling on cylinders [13, 14] has shown quite conclusively that the rapidly moving waves which occur in boiling and which tend to collapse are of the most susceptible wavelength.

The radius R_j of the escaping jet was assumed to be a given fraction a of the wavelength λ. Thus

$$\frac{A_j}{A_h} = \frac{\pi R_j^2}{\lambda^2} = \pi a^2 \tag{9}$$

Zuber guessed that a should be $^1/_4$ so his A_j/A_h was $\pi/16$. The wavelength of disturbances in the jet was taken to be equal to

[4] These expressions were derived by Bellman and Pennington [12].

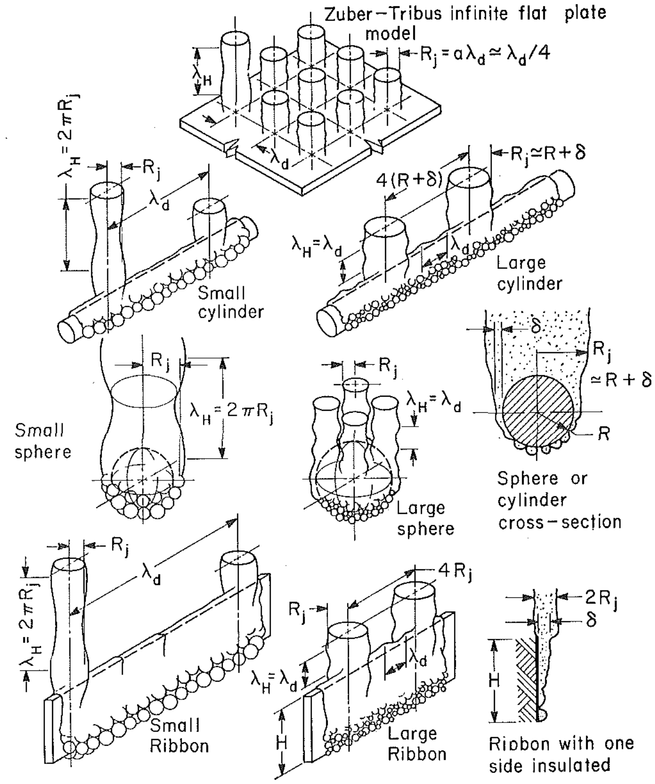

Fig. 1 Vapor-removal configurations near the peak heat flux on a variety of heaters

the length of the Rayleigh unstable wave. This choice was reasonable since this sort of disturbance will occur naturally in any gas jet moving through a liquid. The wavelength λ_H of Rayleigh waves is equal to the circumference of the jet in which they occur, [10] page 473, $2\pi R_j$ or $2\pi a\lambda$. Using this result and equation (9) in equation (6) gives

$$\left.\frac{q_{\max}}{q_{\max F}}\right|_{\text{flat plate}} = \frac{24a^{3/2}}{\sqrt{2\pi}} \cdot \frac{1}{1 \text{ or } \sqrt[4]{3}} \tag{10}$$

Using $a = {}^1/_4$, Zuber obtained for the flat plate

$$q_{\max}|_{\text{flat plate}} = 1.196\, q_{\max F} \quad \text{or} \quad 0.909\, q_{\max F}$$

depending upon whether the correct λ was λ_c or λ_d. He compromised and took equation (2) as a good mean value.

Horizontal Cylinder. The peak heat flux on any finite body will be determined by the configuration of jets above the body since all of the vapor generated below will eventually find its way around the body and up into this jet system. This process is shown schematically for several finite heaters in Fig. 1. The peak heat flux is reached on the body as a whole when these over-

Nomenclature

A_h = area of heater

A_j = cross-sectional area of vapor jets escaping from A_h

a = R_j/λ_d for flat-plate heater

$f(\ )$ = any function of ( )

g = actual gravity (or body) force acting on heater

g_e = earth-normal gravity

h_{fg} = latent heat of vaporization

H = vertical dimension of horizontal ribbon

L = characteristic dimension (= H or R in certain present applications)

P = length of perimeter of cross section of long slender heater

$q_{\max}$ = peak nucleate pool-boiling heat flux

$q_{\max F}$ = characteristic heat flux defined by equation (2), equal to Zuber's prediction for infinite horizontal flat plates

R = radius of cylindrical or spherical heater

R_j = radius of escaping vapor jet

U_H = vapor velocity in jet, for which jet becomes Helmholtz unstable

δ = vapor-blanket thickness

Δ = $\delta\sqrt{g(\rho_f - \rho_g)/\sigma}$

λ = any wavelength in vapor–liquid interface

λ_c = minimum Taylor unstable wavelength, equation (7)

λ_d = most rapidly collapsing Taylor wavelength, $\sqrt{3}\lambda_c$

λ_H = Helmholtz unstable wavelength

ρ_f, ρ_g = saturated liquid and vapor densities

σ = surface tension between liquid and its vapor

Superscript

$'$ denotes a length multiplied by $\sqrt{g(\rho_f - \rho_g)/\sigma}$

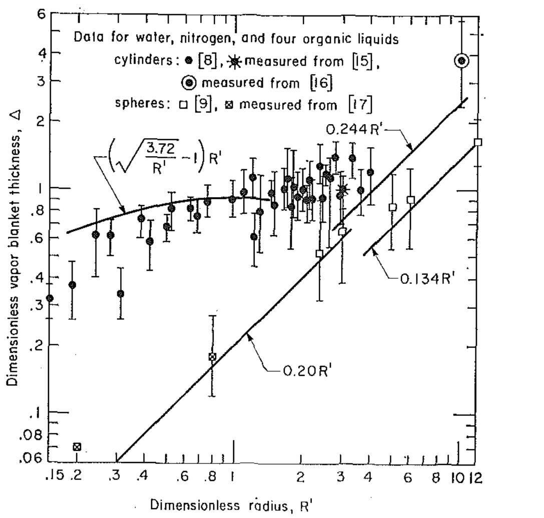

Fig. 2 Vapor-blanket thickness measured on spheres and cylinders

head jets become unstable. Both the configuration and the size of these jets will be determined by the size and shape of the body.

In the specific case of horizontal cylinders—at least on the larger ones—photographic evidence [8] indicates that the jets adjust approximately to the width of the cylinder (plus the thickness of the vapor blankets, 2δ) as shown in Fig. 1. If the wire is small the jets will be small and the spacing can reasonably be assumed equal to λ_d. As the wire increases in size the spacing must eventually spread to beyond λ_d to accommodate jets which now exceed $\lambda_d/2$ in diameter. Sun showed that the spacing was about two jet diameters or about $4(R + \delta)$ in this case. Thus

$$\left.\frac{A_j}{A_h} \simeq \frac{(R+\delta)^2}{2R\lambda_d}\right|_{\substack{\text{small}\\\text{cyls.}}} \qquad \left.\frac{A_j}{A_h} \simeq \frac{R+\delta}{8R}\right|_{\substack{\text{large}\\\text{cyls.}}} \tag{11}$$

Of course equations (11) are true only insofar as $R_j \simeq R + \delta$.

Furthermore, the wavelength λ_d is the dominant disturbance in the interface between the jets on large wires and it is picked up by the jets. The Rayleigh disturbance $2\pi R_j$ is longer than λ_d and would normally become Helmholtz unstable at lower vapor velocities U_H. However, photographic evidence confirmed that vapor jets on large wires were much too short to have collapsed by virtue of the Rayleigh disturbance. This means that the shorter waves of length λ_d are already well developed at the outset, while the Rayleigh waves require some distance to develop. Accordingly, Sun used $\lambda_H = 2\pi R_j \simeq 2\pi(R + \delta)$ for the small cylinders and $\lambda_H = \lambda_d$ for the large ones. Using these λ_H's and equation (11) in equation (6), and using R' to denote L' based on $L = R$, gives

$$\left.\frac{q_{\max}}{q_{\max_F}} = \frac{6}{\pi^2\sqrt{3}}\,\frac{(R'+\Delta)^{3/2}}{R'}\right|_{\substack{\text{small}\\\text{cyls.}}} \quad \text{and} \quad \left.\frac{3^{3/4}}{\pi}\,\frac{R'+\Delta}{R'}\right|_{\substack{\text{large}\\\text{cyls.}}} \tag{12}$$

where $\Delta \equiv \delta\sqrt{g(\rho_f - \rho_g)/\sigma}$, a dimensionless blanket thickness. The transition between small and large cylinders occurs somewhere in the neighborhood of $\lambda_d = 4(R + \delta)$ or $R' \simeq 2.5$, depending on the magnitude of δ.

The parameter R', which has been variously named the "Laplace number," the "Rayleigh number," and the square root of the "Bond number," characterizes the ratio of buoyant forces to capillary forces in a system. As R' becomes very large the system should approach a state in which it is no longer subject to capillary forces. In this state we would expect to see no further influence of R' upon $q_{\max}/q_{\max_F}$, in much the same way as the Reynolds number ceases to exert an influence on the drag coefficient when it becomes sufficiently large. This is what was found to be the case in [8]. As R' became large, Sun measured $\delta \simeq 0.233\,R$, so equation (11) gave $A_j/A_h \simeq 0.155$, and $q_{\max}/q_{\max_F}$ approached a constant value of 0.894.

For small cylinders Sun approximated the measured values of δ with a fairly complicated equation in the form $\Delta = \Delta(R')$. Substitution of this expression in equation (12) gave

$$\left.\frac{q_{\max}}{q_{\max_F}}\right|_{\substack{\text{small}\\\text{cyls. [8]}}} = 0.89 + 2.27\exp\left(-3.44\sqrt{R'}\right) \tag{13}$$

which fit approximately 900 data from a large variety of sources.

Sphere. Photographic observation of boiling on spheres [9] shows a difference between large and small R' behavior just as it did for cylinders. For small spheres a single jet of radius $R_j \simeq R + \delta$ rises as shown in Fig. 1. But when the diameter $2R$ reaches roughly λ_d or $R' \simeq 5.5$, the vapor begins to escape alternately around opposing sides of the sphere in a 4-jet pattern as shown in Fig. 1. Once again visual evidence supports the assumption that $\lambda_H = 2\pi R_j$ for small spheres and $\lambda_H = \lambda_d$ for large ones. Thus

$$\left.\frac{q_{\max}}{q_{\max_F}}\right|_{\substack{\text{small}\\\text{spheres}}} = \frac{24}{\pi\sqrt{R_j'}}\,\frac{A_j}{A_h} \qquad \left.\frac{q_{\max}}{q_{\max_F}}\right|_{\substack{\text{large}\\\text{spheres}}} = \frac{24}{\pi\sqrt[4]{3}}\,\frac{A_j}{A_h} \tag{14}$$

where $R_j' \equiv R_j\sqrt{g(\rho_f - \rho_g)/\sigma}$.

At this point Ded [9] used a notion from this paper to evaluate the unknown area ratio which involves δ. This method is essential to the subsequent developments in this study and we shall take it up next.

Evaluations of A_j/A_h in the $q_{\max}/q_{\max_F}$ Formulae

As a first step to determining A_j/A_h we shall offer a hypothesis that the speed of the vapor passing through the blanket equals that in the escaping jet. For the speeds to differ would require the existence of both pressure differences within the vapor escape path and significant dissipative mixing processes in the jet. We do not believe it is reasonable to look for either, and therefore assume that δ simply adjusts to give equal velocities in both passages.

For the large cylinder, this assumption combined with a simple continuity statement (velocity times cross-sectional area is constant) gives

$$2[4(R+\delta)\delta] = \tfrac{1}{2}A_j \tag{15}$$

and for any sphere it gives

$$2\pi(R+\delta/2)\delta = \tfrac{1}{2}A_j \tag{16}$$

For the small cylinder such a balance is not feasible since the vapor must flow horizontally in a long annulus subject to pressure drops. But for the small sphere equation (16) will still be true. From this point two paths can be followed.

The path followed in [8] was to assume a jet configuration in terms of δ and then to complete the derivation using observed values of δ; [8] and [9] give the needed measurements of δ for both cylinders and spheres as scaled from photographs. These data and two additional points scaled from photographs in other papers [15, 16, 17] are combined in Fig. 2. Approximate lines have been fitted through the data in both the large and small R' ranges. The results are

$$\Delta_{\text{small cylinders}} = \left(\sqrt{3.72/R'} - 1\right)R' \tag{17}$$ [5]

$$\Delta_{\text{large cylinders}} = 0.244\,R' \tag{18}$$ [6]

$$\Delta_{\text{small spheres}} = 0.20\,R' \tag{19}$$

[5] Sun used a more complex fit to the data, one which fit well in the mid-range but was very nearly equal to equation (17) for $R' \leq 1$. We are presently more interested in low-R' behavior than in transitional behavior at higher R'.

[6] This result is a little higher than Sun's and represents a slightly better fit.

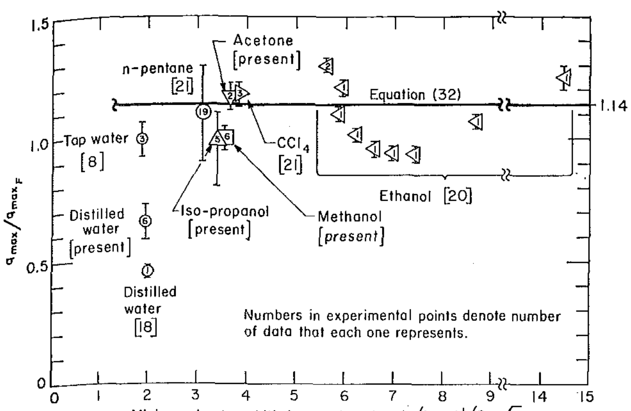

Fig. 3 q_{max} **on broad flat-plate heaters with vertical side walls**

$$\Delta_{\text{large spheres}} = 0.134\, R' \tag{20}$$

Using these equations in equations (15) and (16) leads to

$$\left.\frac{A_j}{A_h}\right|_{\substack{\text{large}\\\text{cyls.}}} = 0.155 \tag{21}$$

$$\left.\frac{A_j}{A_h}\right|_{\substack{\text{large}\\\text{spheres}}} = 0.143 \tag{22}$$

$$\left.\frac{A_j}{A_h}\right|_{\substack{\text{small}\\\text{spheres}}} = 0.220 \tag{23}$$

Ded put equation (22) in equation (14) and obtained

$$\left.\frac{q_{max}}{q_{max_F}}\right|_{\substack{\text{large}\\\text{spheres}}} = 0.84 \tag{24}$$

which differs by 7 percent from the large R' limit of equation (13) for cylinders.

The other approach is to combine the description of the assumed configuration of the jets with equations (15) and (16), solve the result for δ, and then obtain q_{max}/q_{max_F} from equation (12). This is reasonably safe to do in the case of large cylinders since the physical model ($R_j = R + \delta$) is consistent with Sun's photographs. The result is $\delta = 0.244\, R$, which corresponds precisely with the experimental value given in equation (18) and which leads to

$$\left.\frac{q_{max}}{q_{max_F}}\right|_{\substack{\text{large}\\\text{cyls.}}} = 0.904 \tag{25}$$

This is negligibly higher than Sun's result of 0.894, and it is a completely theoretical expression. While this result is accurate, the minor errors in the assumed characteristics of the vapor-escape configuration accumulate more than we would like in other cases. Such errors are particularly troublesome for the small heater configurations.

For small heaters we shall therefore revert to the first approach. In general λ_H should be replaced by $2\pi R_j$ in equation (6), where $R_j = \sqrt{(A_h/\pi)(A_j/A_h)}$. Thus

$$\left.\frac{q_{max}}{q_{max_F}}\right|_{\substack{\text{small}\\\text{heaters}}} = \frac{24}{\pi}\sqrt[4]{\frac{\pi}{A_h}\,\frac{\sigma}{g(\rho_f - \rho_g)}}\left(\frac{A_j}{A_h}\right)^{3/4} \tag{26}$$

If the heater is long and slender, A_h is equal to the product of the cross-sectional perimeter P times λ_d (cf. Fig. 1) and equation (26) becomes

$$\left.\frac{q_{max}}{q_{max_F}}\right|_{\substack{\text{long slender}\\\text{heaters}}} = \frac{24}{\pi\sqrt[8]{12}\,\sqrt[4]{P'}}\left(\frac{A_j}{A_h}\right)^{3/4} = \frac{5.62}{\sqrt[4]{P'}}\left(\frac{A_j}{A_h}\right)^{3/4} \tag{27}$$

Thus for spheres ($A_h = 4\pi R^2$) equations (26) and (23) give

$$\left.\frac{q_{max}}{q_{max_F}}\right|_{\substack{\text{small}\\\text{spheres}}} = \frac{1.734}{\sqrt{R'}} \tag{28}$$

For small cylinders A_j/A_h is approximately $(R + \delta)^2/2R\lambda_d$. Thus under the substitution of equation (17) we obtain

$$\left.\frac{A_j}{A_h}\right|_{\substack{\text{small}\\\text{cyls.}}} = 0.171 \tag{29}$$

Substituting equation (29) and $P' = 2\pi R'$ in equation (27) then gives

$$\left.\frac{q_{max}}{q_{max_F}}\right|_{\substack{\text{small}\\\text{cyls.}}} = \frac{0.94}{\sqrt[4]{R'}} \tag{30}$$

q_{max}/q_{max_F} for Flat Plates

A number of suggestions as to how one might improve Zuber's prediction of q_{max} for the flat plate have arisen in the preceding section. For one thing, Sun's large-cylinder model, based on the presumption that the jet spacing cannot be less than $4R_j$, was highly successful. Furthermore his corresponding assumption that $\lambda_H = \lambda_d$ in this case was also justified by the success of the result. We shall adapt these ideas to the flat plate by agreeing with Zuber that R_j equals $^1/_4$ of the jet spacing without *saying precisely what that spacing is.*[7] *Then we shall use* λ_d *for* λ_H. Then equation (9) gives

$$\left.\frac{A_j}{A_h}\right|_{\substack{\text{flat}\\\text{plate}}} = \frac{\pi}{16} \tag{31}$$

and equation (6) gives

$$\left.\frac{q_{max}}{q_{max_F}}\right|_{\substack{\text{flat}\\\text{plate}}} = \frac{24}{\pi}\sqrt{\frac{2\pi}{2\pi\sqrt{3}}\,\frac{\pi}{16}} = 1.14 \tag{32}$$

Of course an important point relative to Zuber's equation is that it was never systematically tested against data obtained in the configuration for which it was intended. To approximate an infinite flat plate experimentally one must first employ a very clean finite plate, much larger in size than λ_d. Then he must employ vertical side walls to prevent a horizontal inflow of liquid, since this has been shown [18, 19] to seriously influence q_{max}.

The data that we have located which meet these criteria are few. The vast majority of available flat-plate data were obtained with strip or disk heaters in open pools, and are hence unusable. The classical data of Cichelli and Bonilla [20] are for the correct configuration—a $3^3/_4$-in-dia disk heater which formed the bottom of a cylindrical container for the boiled liquid. A great many of their data must be eliminated because they were obtained on "dirty" heaters. Most of the remainder are for nominal fluids of extremely low purity—actually mixtures for which properties are not known and correlations cannot be applied. Only a few of their data for ethanol remain for use. Berenson presented similar data for CCl_4 and n-pentane on 2-in-dia heaters that were subject to very close control of surface condition.

Costello et al. [18] also presented data for a 2-in-wide plate heater in water with side walls, but their data raise more questions than they resolve. Their q_{max} for "tap water" is close to q_{max_F}, but their result for distilled water in a very clean system is lower by a factor of 0.4. No satisfactory explanation is given for this startling result.

Figure 3 gives these data. It also includes additional preliminary flat-plate data which we shall present informally at this

[7] It was shown in [14] that while λ_d is favored, it is favored only very slightly over a broad span of neighboring Taylor wavelengths.

time. They were obtained on a clean smooth copper plate 2.5 in. in diameter as part of another study which has not yet been completed. The existing data are limited in number and scope, and more are needed for other liquids and larger values of L'. However, equation (32) has been included in the figure and it agrees, about as well as any line could, with the existing data.

The fact that our distilled-water data for $L/\lambda_d \simeq 2$ are low (as was Costello's point) suggests that this might represent a peculiarity of the vapor-jet configuration. It is possible that only one jet can be accommodated on the heater when $L/\lambda_d = 2$, while one just slightly larger will accommodate three jets. As L/λ_d increases this kind of fluctuation will decrease rapidly.

Some General Inferences Concerning Hydrodynamic Predictions of q_{max}

At this point it is advantageous to summarize our major findings:

1 $\dfrac{q_{max}}{q_{maxF}} = \dfrac{24}{\pi} \sqrt[4]{\dfrac{\pi}{A_h} \dfrac{\sigma}{g(\rho_f - \rho_g)}} \left(\dfrac{A_j}{A_h}\right)^{3/4}$ for small heaters, equation (26).

2
$$\frac{q_{max}}{q_{maxF}} = \frac{24}{\pi\sqrt[4]{3}} \frac{A_j}{A_h} \quad \text{for large heaters} \tag{33}$$

3 $\lambda_H = 2\pi R_j$ for small heaters.

4 $\lambda_H = \lambda_d$ for large heaters including the flat plate.

5 For small bluff bodies $A_h \sim L^2$ and equation (26) gives

$$\frac{q_{max}}{q_{maxF}} = \frac{\text{constant}}{\sqrt{L'}} \tag{34}$$

where the constant must be determined experimentally because A_j/A_h is only known in one configuration (small spheres).

6 Except for the case of small spheres and infinite flat plates, A_j/A_h seems to be a constant, very nearly independent of configuration. For the known cases (within about 10 percent)

$$\frac{A_j}{A_h} \simeq 0.155 \tag{35}$$

7 Therefore, from equation (14),

$$\left.\frac{q_{max}}{q_{maxF}}\right|_{\substack{\text{large}\\\text{heaters}}} \simeq 0.9 \tag{36}$$

8 For the infinite flat plate

$$\left.\frac{q_{max}}{q_{maxF}}\right|_{\substack{\text{flat}\\\text{plate}}} = 1.14 \tag{37}$$

9 From equations (27) and (35)

$$\left.\frac{q_{max}}{q_{maxF}}\right|_{\substack{\text{long slender}\\\text{heaters}}} \simeq \frac{1.4}{\sqrt[4]{P'}} \tag{38}$$

Equation (30) is very close to being a special case of equation (38), since $0.94/\sqrt[4]{R'} = 1.48/\sqrt[4]{P'}$ when $2\pi R = P$. The 6 percent difference between 1.48 and 1.40 is within the scatter of the experimental data.

10 The transition between large and small heater behavior occurs about where the breadth of the heater is on the order of λ_d, typically where R' is on the order of 5. Past experience [8, 9] indicates that the appropriate forms of equations (26) and (33) can simply be extrapolated to their point of intersection to obtain a continuous prediction.

Of the preceding items, numbers 5, 6, 7, 8, and 10 have been thoroughly validated with data, [8, 9] and the present study, except insofar as item 7 might require further experimental verification and item 5 has only been verified in one configuration. Item 9 is a fairly solid conjecture that should be verified. Items 1–4 and the generalization in 5 have been verified experimentally only in the sense that their overall consistency with data and their self-consistency have been carefully checked.

Illustrative Application: Prediction of q_{max} on Horizontal Vertically Oriented Ribbons and Experimental Verification

Consider next the case of a thin horizontal ribbon heater with the broad side oriented vertically, as shown at the bottom of Fig. 1. We shall also give brief attention to such a ribbon with one side insulated. Items 2, 6, and 7 apply to either of these cases as long as H is large.

When H is small equation (38) should apply to either insulated or uninsulated ribbons as long as the right P' is used.

Table 1 includes original data for vertically oriented ribbon heaters in four liquids: acetone, benzene, methanol, and isopropanol. The ribbons were all of nichrome, 0.009 in. thick and about 4 in. in length, and they varied in height H from 0.041 in. to 0.188 in. They were operated as electrical-resistance heaters and were connected to the heavy power supply electrodes through brass-ribbon attachments which served to prevent vapor hangup by providing a smooth transition section. The range of H' $(\equiv H\sqrt{g(\rho_f - \rho_g)/\sigma})$ was greatly increased by observing q_{max} in the University of Kentucky Gravity Boiling Centrifuge Facility, at both elevated gravity and earth-normal gravity g_e.

Complete details of the experimental method and apparatus can be obtained from [8, 22], since exactly the same equipment and procedure were employed. The probable experimental error in q_{max} was about ± 4 percent, although intrinsic variability of the data was $\simeq\pm 15$ percent which is typical for such results. All ribbons had a smooth cold-rolled finish (as delivered). Before each test the ribbons were carefully washed in soap and hot water, and then rinsed in the test fluid.

We can be sure that, even on these small ribbons, q_{max} did not occur prematurely by virtue of low-thermal-capacity effects such as Houchin [23] observed, since he was only able to observe the phenomenon in water. Even though he used much thinner ribbons than we, he never witnessed the early burnout in organic liquids.

These data are presented in dimensionless form in Fig. 4.

Table 1 Peak heat flux on vertically oriented horizontal ribbon

fluid	H (in.)	g/g_e	q_{max} $\frac{\text{Btu}}{\text{ft}^2\,\text{hr}}$	H'	$\frac{q_{max}}{q_{maxF}}$
Acetone	0.041	1	142,000 ± 5000	0.65	1.34
	0.051	1	156,000 ± 6000	0.80	1.47
	0.080	1	118,000 ± 3000	1.27	1.12
	0.1395	1	107,000 ± 3000	2.207	1.01
	0.188	1	98,000 ± 3000	2.98	0.925
	0.144	4.01	141,000 ± 1000	4.56	0.94
		8.30	165,000 ± 2000	6.56	0.92
		17.84	226,000 ± 1000	9.62	1.03
		32.32	268,000 ± 4000	12.95	1.06
		49.49	305,000 ± 3000	16.03	1.03
Benzene	0.041	1	126,000 ± 2000	0.635	1.31
	0.055	1	118,000 ± 4000	0.85	1.23
	0.0855	1	96,000 ± 3000	1.32	1.00
	0.144	4.01	135,000 ± 2000	2.65	0.99
		7.98	165,500 ± 2500	3.70	1.02
		18.32	203,000 ± 3000	5.60	1.02
		31.68	237,000 ± 2000	7.35	1.03
		49.49	272,000 ± 5000	9.25	1.06
Methanol	0.055	1	201,000 ± 4000	0.88	1.19
	0.099	1	161,000 ± 3000	1.59	0.95
	0.1395	1	140,000 ± 4000	2.25	0.83
	0.188	1	124,000 ± 4000	3.03	0.74
	0.144	4.01	182,000 ± 6000	4.63	0.75
		7.98	221,500 ± 1500	6.54	0.78
		18.32	282,000 ± 8000	9.91	0.80
		32.32	314,000 ± 8000	13.16	0.77
Isopropanol	0.1395	1	101,000 ± 3000	2.34	0.76
	0.188	1	90,000 ± 4000	3.16	0.74
	0.144	4.11	153,000 ± 5000	4.90	0.81
		8.3	180,000 ± 7000	6.96	0.80
		18.56	210,000 ± 2000	10.40	0.76
		32.32	255,000 ± 6000	13.74	0.81

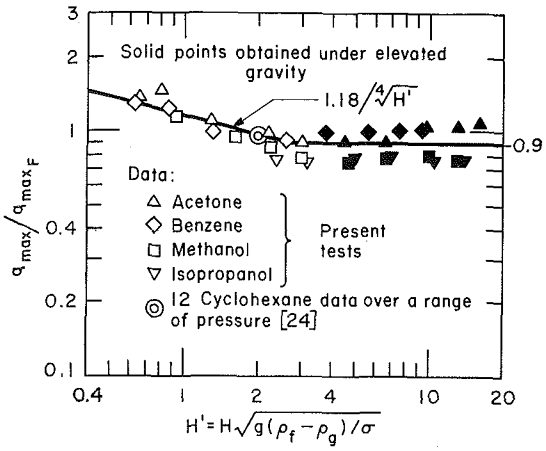

Fig. 4 q_{max} **on horizontal ribbon heaters oriented vertically**

Following the prescription in the preceding section we represent the data for large L' using equation (36)

$$\left.\frac{q_{max}}{q_{maxF}}\right|_{\substack{\text{large}\\ \text{horiz. ribbons}\\ \text{vert. orient.}}} = 0.9 \qquad (36)$$

And for the range of small H' we use equation (38) with $P' = 2H'$. The result is

$$\left.\frac{q_{max}}{q_{maxF}}\right|_{\substack{\text{small}\\ \text{horiz. ribbons}\\ \text{vert. orient.}}} = \frac{1.18}{\sqrt[4]{H'}} \qquad (39)$$

The correlation is well within the typical scatter for such data. The division between large and small heaters occurs at $H' \simeq 2.7$ in this case.

The peak heat flux was also measured on two 0.009-in-thick horizontal nichrome ribbons, vertically oriented but with one side heavily insulated with Sauereisen cement. A 0.099-in. ribbon was observed in methanol and a 0.188-in. ribbon was observed in acetone. The results were

$$\text{at} \quad H' = 1.59 \qquad 1.19 \leq \frac{q_{max}}{q_{maxF}} \leq 1.30$$

$$\text{at} \quad H' = 2.98 \qquad 1.03 \leq \frac{q_{max}}{q_{maxF}} \leq 1.07$$

respectively. These data are plotted in Fig. 5 along with some high-gravity data given by Adams [25] for higher values of H' in the same geometry.

In this case Adams' data fit the limiting value

$$\left.\frac{q_{max}}{q_{maxF}}\right|_{\substack{\text{large}\\ \text{horiz. ribbon}\\ \text{vert. orient.}\\ \text{1 side insul.}}} = 0.90 \qquad (36)$$

almost perfectly. For small heaters $P' = H'$ and

$$\left.\frac{q_{max}}{q_{maxF}}\right|_{\substack{\text{small}\\ \text{horiz. ribbon}\\ \text{vert. orient.}\\ \text{1 side insul.}}} = \frac{1.4}{\sqrt[4]{H'}} \qquad (40)$$

Both equations (36) and (40) correspond with $A_j/A_h = 0.155$. The transition from large to small H' occurs at 6 when the ribbon is insulated and at 2.6 when it is not.

Conclusions

1 The method of hydrodynamic prediction of the peak heat flux on finite heaters is discussed in detail and certain general guidelines are set up for making such predictions. The assumption that the vapor velocities in the vapor blanket and in the jets must match greatly streamlines prior descriptions and simplifies these guidelines. The guidelines are spelled out in the section "Some General Inferences Concerning Hydrodynamic Predictions of q_{max}."

2 The peak heat flux on an infinite flat plate is 1.14 q_{maxF}, but there is a need for more data in verification of this result.

3 The peak heat fluxes for large and small horizontal ribbons vertically oriented, with and without insulation on one side, are given by equations (36), (39), and (40).

4 The existing hydrodynamic q_{max} predictions for finite bodies are summarized in Fig. 6. The figure includes an indication of the number of data by which each has been verified. This number exceeds the number of points actually shown in Figs. 4 and 5, since more than one observation has been lumped in some of the points. The curves have all been terminated at $L' = 0.1$ on the left side, since hydrodynamic predictions are known to deteriorate for $L' \lessapprox 0.1$, see [8, 26].

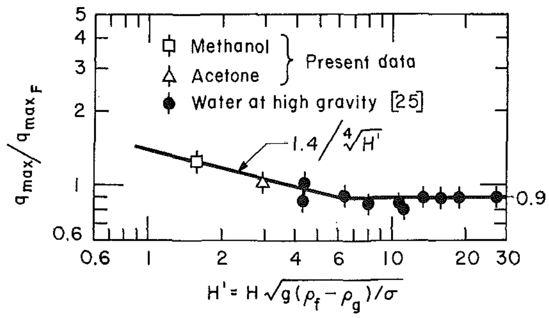

Fig. 5 q_{max} **on horizontal ribbon heaters oriented vertically with one side insulated**

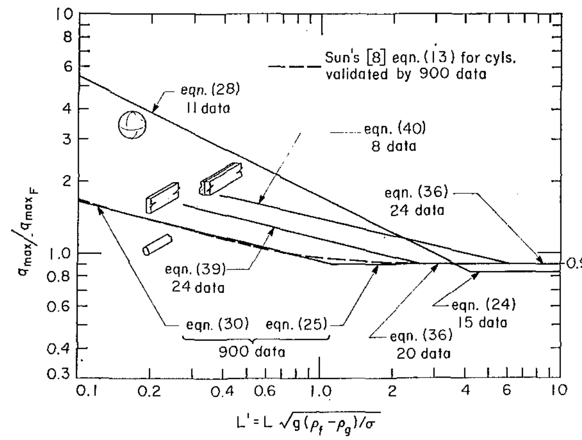

Fig. 6 Collected predictions of q_{max} **for four finite heater configurations**

References

1 Zuber, N., "Hydrodynamic Aspects of Boiling Heat Transfer," AEC Report No. AECU-4439, Physics and Mathematics, 1959.

2 Zuber, N., Tribus, M., and Westwater, J. W., "The Hydrodynamic Crisis in Pool Boiling of Saturated and Subcooled Liquids," *International Developments in Heat Transfer*, ASME, New York, N. Y., 1963, pp. 230–236.

3 Kutateladze, S. S., "On the Transition to Film Boiling under Natural Convection," *Kotloturbostroenie*, No. 3, 1948, p. 10.

4 Bobrovich, G. I., Gogonin, I. I., Kutateladze, S. S., and Moskvicheva, V. N., "The Critical Heat Flux in Binary Mixtures," *Jour. Appl. Mech. and Tech. Phys.*, No. 4, 1962, pp. 108–111.

5 Bobrovich, G. I., Gogonin, I. I., and Kutateladze, S. S., "Influence of Size of Heater Surface on the Peak Pool Boiling Heat Flux," *Jour. Appl. Mech. and Tech. Phys.*, No. 4, 1964, pp. 137–138.

6 Lienhard, J. H., and Watanabe, K., "On Correlating the Peak and Minimum Boiling Heat Fluxes With Pressure and Heater Configuration," JOURNAL OF HEAT TRANSFER, TRANS. ASME, Series C, Vol. 88, No. 1, Feb. 1966, pp. 94–100.

7 Lienhard, J. H., "Interacting Effects of Gravity and Size upon the Peak and Minimum Pool Boiling Heat Fluxes," NASA CR-1551, May 1970.

8 Sun, K. H., and Lienhard, J. H., "The Peak Pool Boiling Heat Flux on Horizontal Cylinders," *International Journal of Heat and Mass Transfer*, Vol. 13, 1970, pp. 1425–1439.

9 Ded, J. S., and Lienhard, J. H., "The Peak Pool Boiling from a Sphere," *AIChE Journal*, Vol. 18, No. 2, Mar. 1972, pp. 337–342.

10 Lamb, H., *Hydrodynamics*, 6th ed., Dover, New York, N. Y., 1945.

11 Dhir, V., "Some Notes on the Development of the Hydrodynamic Theory of Boiling," University of Kentucky Tech. Report No. 19-70-ME6, Mar. 1970.

12 Bellman, R., and Pennington, R. H., "Effects of Surface Tension and Viscosity on Taylor Instability," *Quart. App. Math.*, Vol. 12, 1954, pp. 151–162.

13 Lienhard, J. H., and Wong, P. T. Y., "The Dominant Unstable Wavelength and Minimum Heat Flux During Film Boiling on a Horizontal Cylinder," JOURNAL OF HEAT TRANSFER, TRANS. ASME, Series C, Vol. 86, No. 2, May 1964, pp. 220–226.

14 Lienhard, J. H., and Sun, K.-H., "Effects of Gravity and Size Upon Film Boiling From Horizontal Cylinders," JOURNAL OF HEAT TRANSFER, TRANS. ASME, Series C, Vol. 92, No. 2, May 1970, pp. 292–298.

15 Westwater, J. W., and Santangelo, J. G., "Photographic Study of Boiling," *Ind. Engr. Chem.*, Vol. 47, 1955, p. 1605.

16 Costello, C. P., and Adams, J. M., "The Interrelation of Geometry, Orientation and Acceleration in the Peak Heat Flux Problem," Mechanical Engineering Department Report, University of Washington, Seattle, Wash., c. 1963.

17 Hendricks, R. C., private communication of unpublished data related to the paper by Hendricks and Baumeister, "Film Boiling from Submerged Spheres," NASA TN D-5124, June 1969.

18 Costello, C. P., Bock, C. O., and Nichols, C. C., "A Study of Induced Convective Effects on Pool Boiling Burnout," *CEP Symposium Series*, Vol. 61, 1965, pp. 271–280.

19 Lienhard, J. H., and Keeling, K. B., Jr., "An Induced-Convection Effect Upon the Peak-Boiling Heat Flux," JOURNAL OF HEAT TRANSFER, TRANS. ASME, Series C, Vol. 92, No. 1, Feb. 1970, pp. 1–5.

20 Cichelli, M. T., and Bonilla, C. F., "Heat Transfer to Liquids Boiling under Pressure," *Trans. AIChE*, Vol. 41, 1945, p. 755.

21 Berenson, P. J., "Transition Boiling Heat Transfer from a Horizontal Surface," M.I.T. Heat Transfer Laboratory Technical Report No. 17, 1960.

22 Sun, K. H., "The Peak Pool Boiling Heat Flux on Horizontal Cylinders," MS thesis, University of Kentucky, 1969 (available as College of Engineering Bulletin No. 88, May 1969).

23 Houchin, W. R., and Lienhard, J. H., "Boiling Burnout in Low Thermal Capacity Heaters," ASME Paper No. 66-WA/HT-40.

24 Lienhard, J. H., and Schrock, V. E., "The Effect of Pressure, Geometry, and the Equation of State Upon the Peak and Minimum Boiling Heat Flux," JOURNAL OF HEAT TRANSFER, TRANS. ASME, Series C, Vol. 85, No. 3, Aug. 1963, pp. 261–272.

25 Adams, J. M., "A Study of the Critical Heat Flux in an Accelerating Pool Boiling System," PhD thesis, University of Washington, Seattle, Wash., Sept. 1962 (also released as University of Washington Mechanical Engineering Department Report to NSF, Sept. 1, 1962).

26 Bakhru, N., and Lienhard, J. H., "Boiling from Small Cylinders," to be published in *International Journal of Heat and Mass Transfer*.